



# WMO GREENHOUSE GAS BULLETIN

The State of Greenhouse Gases in the Atmosphere Based on Global Observations through 2020

No. 17 | 25 October 2021

ISSN 2078-0796

Roughly half of the carbon dioxide ( $\text{CO}_2$ ) emitted by human activities today remains in the atmosphere. The rest is absorbed by oceans and land ecosystems. The fraction of emissions remaining in the atmosphere, called airborne fraction (AF), is an important indicator of the balance between sources and sinks. AF varies a lot from year to year, and over the past 60 years the relatively uncertain annual averages have varied between 0.2 (20%) and 0.8 (80%). However, statistical analysis shows that there is no significant trend in the average AF value of 0.42 over the long term (about 60 years) (see Figure 1). This means that only 42% of human  $\text{CO}_2$  emissions remain in the atmosphere. Land and ocean  $\text{CO}_2$  sinks have continued to increase proportionally with the increasing emissions. It is uncertain how AF will change in the future because the uptake processes are sensitive to climate and land-use changes.

Changes in AF will have strong implications for reaching the goal of the Paris Agreement, namely to limit global warming to well below  $2^\circ\text{C}$ , and will require adjustments in the timing and/or size of the emission reduction commitments. Ongoing climate change and related feedbacks, such as more frequent droughts and the connected increased occurrence and intensification of wildfires [2], might reduce  $\text{CO}_2$

uptake by land ecosystems. Ocean uptake might also be reduced as a result of higher sea-surface temperatures, decreased pH due to  $\text{CO}_2$  uptake [3] and the slowing of the meridional ocean circulation due to increased melting of sea ice [4]. Timely and accurate information on changes in AF is critical to detecting future changes in the source/sink balance.

Luckily, information is available from observations of atmospheric  $\text{CO}_2$  made at key locations around the world from the WMO Global Atmosphere Watch (GAW) Programme and its contributing networks. These long-term and accurate observations give direct insight into the trend in atmospheric levels of  $\text{CO}_2$  and other greenhouse gases (GHGs), as illustrated in this and previous editions of the Bulletin. These data can be combined with other observations (for example of stable isotope ratios and the oxygen/nitrogen ( $\text{O}_2/\text{N}_2$ ) ratio) and inverse models (that apply atmospheric tracer transport models) and help derive quantitative information on the strength of major  $\text{CO}_2$  uptake processes in the global carbon cycle and analyse AF and the factors contributing to its changes [5].

Based on this direct observational information, better projections of  $\text{CO}_2$  levels for the expected emission scenarios can be provided, allowing for improved

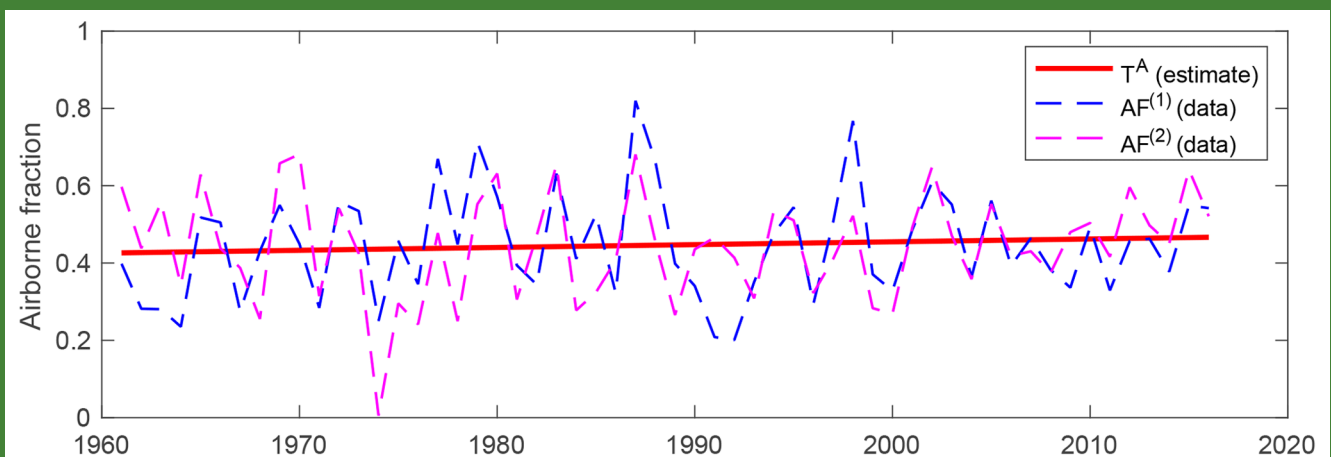


Figure 1. Fitted estimate of the linear trend in AF ( $T^A$ ) over the period 1960–2016 [1]. Individual estimates of annual mean AF are depicted by the dashed lines using two methods with zero ( $\text{AF}^{(1)}$ ) and a non-zero ( $\text{AF}^{(2)}$ ) carbon budget imbalance. The slightly upward slope of the trend over the period is found to be not statistically significant.

climate projections. Figure 2 shows an example of an analysis where long-term observations at a single station can be used to determine the distribution of fossil fuel CO<sub>2</sub> emissions between terrestrial and oceanic sinks, based on the fact that for respiration and photosynthesis CO<sub>2</sub> and O<sub>2</sub> co-vary, whereas for ocean gas exchange they do not. Note that the analysis covers a different period than that for Figure 1 and that it does not include all sources of uncertainty, such as representativeness of the station and calibration uncertainties.

In order to better support GHG management policies through analysis of natural sinks and fossil fuel emissions, and to narrow them down to the regional or the local level, improved sustainability of the current in situ network and additional in situ data are needed. This goes hand in hand with increasing remote sensing capacities, especially in currently undersampled regions, such as Africa and other tropical regions.

The recent 2021 GCOS status report [6] recognizes the recent improvements in availability of observations in for example the GAW GHG network and satellite observations, but also points to four main areas that still need improvements:

- Ensuring the sustainability of observations,
- Addressing gaps in the system,
- Ensuring permanent, free and unrestricted access to the observations,
- Increasing support for policies driven by the UNFCCC Paris Agreement.

The latter point would require more regional observations (in urban and contributing networks like Integrated Carbon Observation System) over the whole globe. WMO GAW contributes to this for example through the IG<sup>3</sup>IS initiative (<https://ig3is.wmo.int/>, see also GHG Bulletin 12) where an international standard for urban GHG monitoring is being developed.

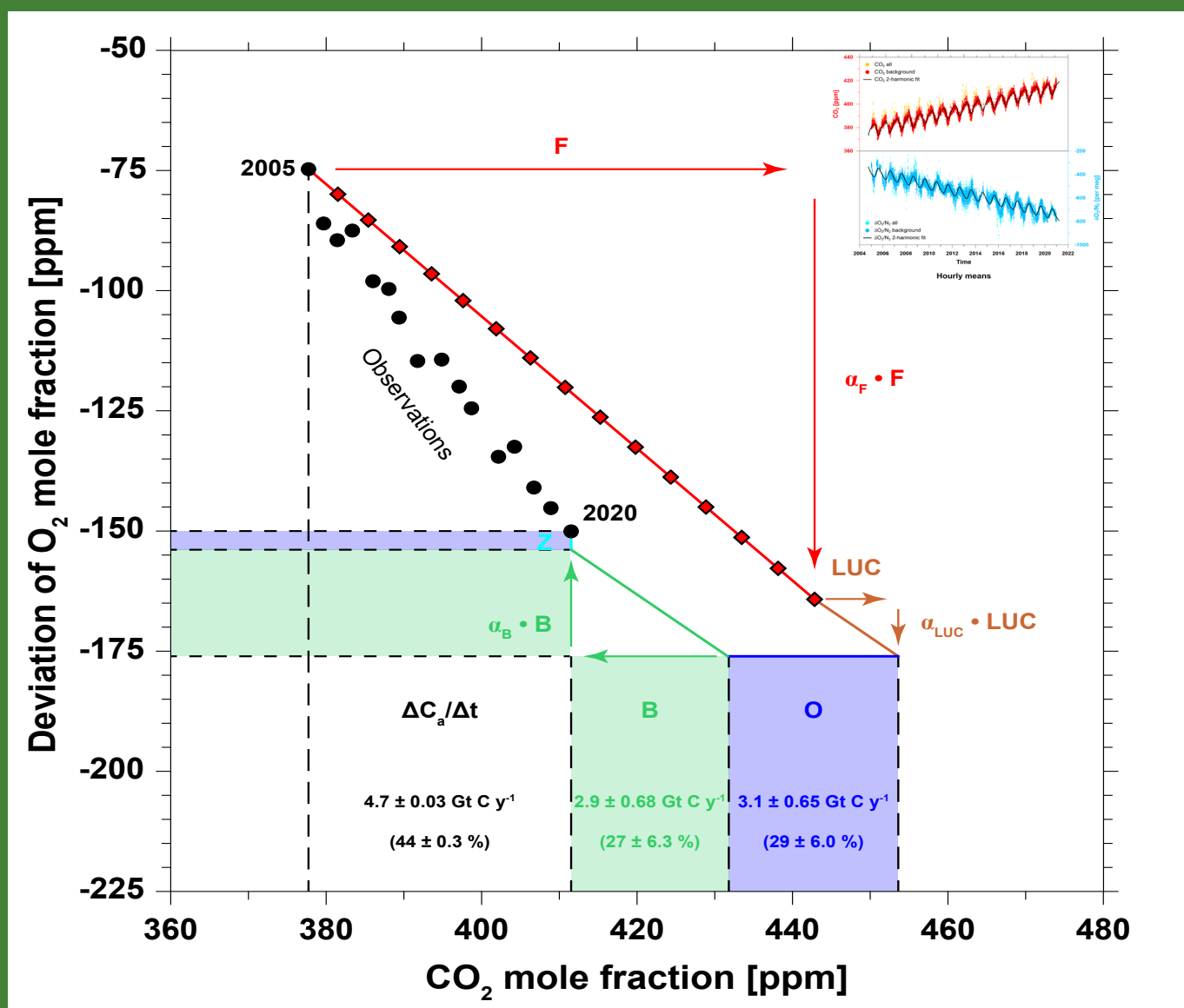


Figure 2. Analysis of the global carbon budget based on observations of CO<sub>2</sub> and O<sub>2</sub> at WMO GAW global station Jungfraujoch, Switzerland [7]. The top-right insert shows the underlying hourly time series for CO<sub>2</sub> and the O<sub>2</sub>/N<sub>2</sub> ratio from 2005 to 2021. The outcome of the analysis shows that over the 16-year period the percentage of emissions remaining in the atmosphere is 44% ( $\Delta C_a/\Delta t = 0.44$ ), global biosphere uptake (B) is 27% and global ocean uptake (O) is 29%. The red line depicts the theoretical changes in CO<sub>2</sub> and O<sub>2</sub> levels in response to fossil fuel emissions (F) and emission associated with land-use change (LUC). (Z) shows changes in O<sub>2</sub> level due to ocean thermal outgassing.

## Executive summary

The latest analysis of observations from the WMO GAW in situ observational network shows that globally averaged surface mole fractions<sup>(1)</sup> for CO<sub>2</sub>, methane (CH<sub>4</sub>) and nitrous oxide (N<sub>2</sub>O) reached new highs in 2020, with CO<sub>2</sub> at 413.2 ± 0.2 ppm<sup>(2)</sup>, CH<sub>4</sub> at 1889 ± 2 ppb<sup>(3)</sup> and N<sub>2</sub>O at 333.2 ± 0.1 ppb. These values constitute, respectively, 149%, 262% and 123% of pre-industrial (before 1750) levels. The increase in CO<sub>2</sub> from 2019 to 2020 was slightly lower than that observed from 2018 to 2019, but higher than the average annual growth rate over the last decade. This is despite the approximately 5.6% drop in fossil fuel CO<sub>2</sub> emissions in 2020 due to restrictions related to the coronavirus disease (COVID-19) pandemic. For CH<sub>4</sub>, the increase from 2019 to 2020 was higher than that observed from 2018 to 2019 and also higher than the average annual growth rate over the last decade. For N<sub>2</sub>O, the increase from 2019 to 2020 was higher than that observed from 2018 to 2019 and also higher than the average annual growth rate over the past 10 years. The National Oceanic and Atmospheric Administration (NOAA) Annual Greenhouse Gas Index (AGGI) [8] shows that from 1990 to 2020, radiative forcing by long-lived greenhouse gases (LLGHGs) increased by 47%, with CO<sub>2</sub> accounting for about 80% of this increase.

## Overview of observations from the GAW in situ observational network for 2020

This seventeenth annual WMO Greenhouse Gas Bulletin reports atmospheric abundances and rates of change of the most important LLGHGs – CO<sub>2</sub>, CH<sub>4</sub> and N<sub>2</sub>O – and provides a summary of the contributions of other GHGs. Those three, together with dichlorodifluoromethane (CFC-12) and trichlorofluoromethane (CFC-11), account for approximately 96%<sup>(4)</sup> [8] of radiative forcing due to LLGHGs (Figure 3).

All percentage contributions to radiative forcing in this Bulletin are calculated following the methodology in [8], use 1750 as a reference period and only include LLGHGs.

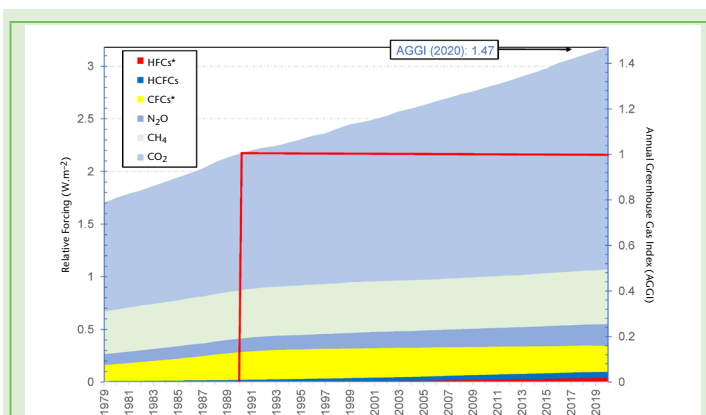


Figure 3. Atmospheric radiative forcing, relative to 1750, by LLGHGs corresponding to the 2020 update of the NOAA AGGI [8]. Note that the updated calculation from the 2021 Intergovernmental Panel on Climate Change (IPCC) Working Group I report [9] has not been included in this estimate. The “CFCs\*” grouping includes other long-lived gases that are not chlorofluorocarbons (CFCs) (e.g. CCl<sub>4</sub>, CH<sub>3</sub>CCl<sub>3</sub> and halons), but the CFCs accounted for the majority (95% in 2020) of this radiative forcing. The “HCFCs” grouping includes the three most abundant hydrochlorofluorocarbons (HCFCs) (HCFC-22, HCFC-141b and HCFC-142b). The “HFCs\*” grouping includes the most abundant hydrofluorocarbons (HFCs) (HFC-134a, HFC-23, HFC-125, HFC-143a, HFC-32, HFC-152a, HFC-227ea and HFC-365mfc) and sulfur hexafluoride (SF<sub>6</sub>) for completeness, although SF<sub>6</sub> only accounted for a small fraction of the radiative forcing from this group in 2020 (13%).

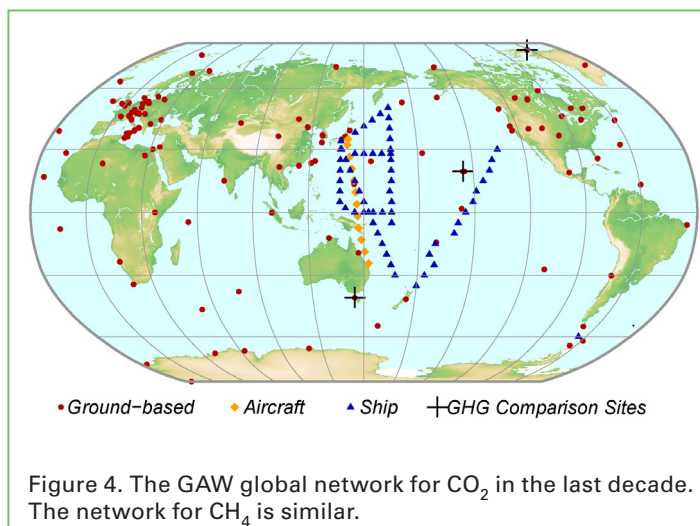


Figure 4. The GAW global network for CO<sub>2</sub> in the last decade. The network for CH<sub>4</sub> is similar.

The WMO GAW Programme coordinates systematic observations and analyses of GHGs and other trace species. Sites where GHGs have been measured in the last decade are shown in Figure 4. Measurement data are reported by participating countries and archived and distributed by the WMO World Data Centre for Greenhouse Gases (WDCGG) at the Japan Meteorological Agency.

The results reported here by WDCGG for the global average and growth rate are slightly different from the results reported by NOAA for the same years [10], owing to differences in the stations used and the averaging procedure, as well as a slight difference in the time period for which the numbers are representative. WDCGG follows the procedure described in detail in GAW Report No. 184 [11]. The results reported here for CO<sub>2</sub> differ slightly from previous Greenhouse Gas Bulletins (by approximately 0.2 ppm) because data are now reported on the new CO<sub>2</sub> calibration scale WMO CO<sub>2</sub> X2019 [12]. Historical data have been converted to the new scale to ensure consistency in reported trends.

The table provides the globally averaged atmospheric abundances of the three major GHGs in 2020 and the changes

Table. Global annual surface mean abundances (2020) and trends of key GHGs from the GAW in situ observational network. Units are dry-air mole fractions, and uncertainties are 68% confidence limits. The averaging method is described in GAW Report No. 184 [11].

	CO <sub>2</sub>	CH <sub>4</sub>	N <sub>2</sub> O
2020 global mean abundance	413.2±0.2 ppm	1889±2 ppb	333.2±0.1 ppb
2020 abundance relative to 1750 <sup>a</sup>	149%	262%	123%
2019–2020 absolute increase	2.5 ppm	11 ppb	1.2 ppb
2019–2020 relative increase	0.61%	0.59%	0.36%
Mean annual absolute increase over the last 10 years	2.40 ppm yr <sup>-1</sup>	8.0 ppb yr <sup>-1</sup>	0.99 ppb yr <sup>-1</sup>

<sup>a</sup> Assuming a pre-industrial mole fraction of 278 ppm for CO<sub>2</sub>, 722 ppb for CH<sub>4</sub> and 270 ppb for N<sub>2</sub>O. The number of stations used for the analyses was 139 for CO<sub>2</sub>, 138 for CH<sub>4</sub> and 105 for N<sub>2</sub>O.

## CarbonWatchNZ: using long-term atmospheric CO<sub>2</sub> measurements to shed light on New Zealand's forest carbon uptake

In New Zealand, forests offset 30% of GHG emissions, but estimates of forest carbon uptake remain highly uncertain. The national inventory report (NIR), which tracks progress against emissions targets under the United Nations Framework Convention on Climate Change (UNFCCC), uses measurements of tree diameter and height at a national network of sites to estimate forest carbon uptake [25]. This approach follows international best practices guidelines [26], but it may not capture all forest ecosystem processes adequately.

Independent estimates from atmospheric CO<sub>2</sub> measurements and modelling suggest that forest carbon uptake may be significantly underestimated by both the NIR and terrestrial biosphere modelling [27]. The most recent results confirm this sink with additional measurements and modelling and show that it has lasted for at least a decade (Figure 10).

This additional carbon uptake occurs in one of the most unlikely places: the south-west of South Island, a region dominated by mature indigenous forests (Figure 11). Indigenous forests in New Zealand have long been thought to absorb less carbon than plantation forestry, which is primarily fast-growing exotic trees. These results could open a new, more sustainable pathway to manage the country's forests for carbon uptake with many environmental co-benefits [27].

New Zealand's Climate Change Commission recently recommended that the country transition away from relying on plantation forestry towards

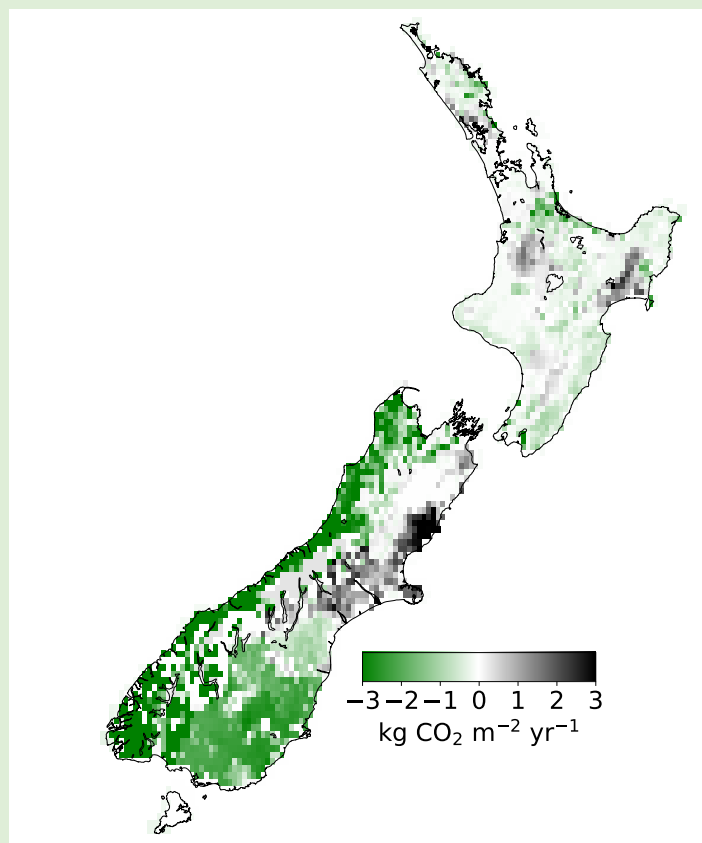


Figure 11. Average uptake of New Zealand's terrestrial biosphere between 2011 and 2020 estimated from atmospheric measurements and modelling.

planting native forests for carbon sequestration. However, little is known about the sensitivity of New Zealand's unique indigenous forests to future climate change. Ongoing measurements will help to understand the sensitivity of these forests to climate change and how their carbon uptake will respond to a changing world.

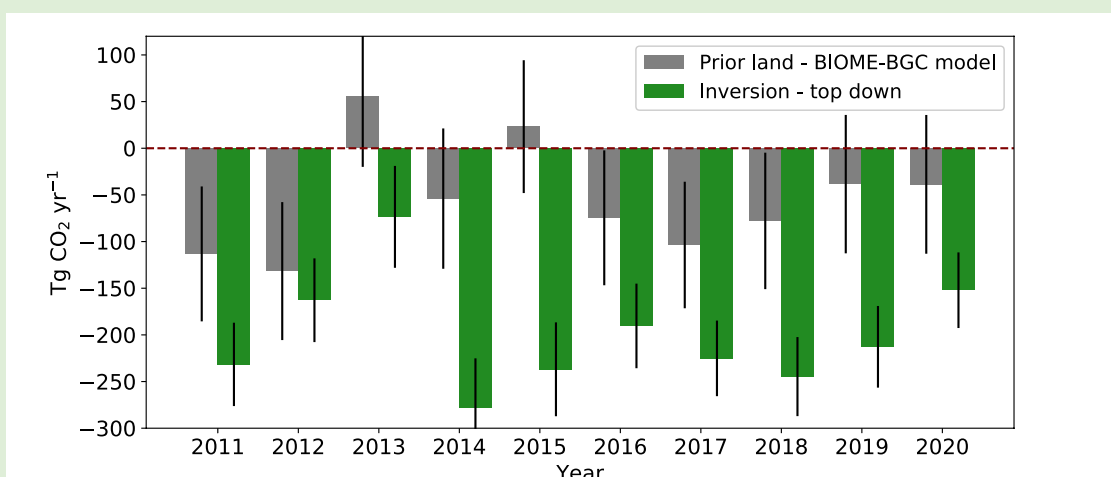


Figure 10. Annual average carbon flux from New Zealand's terrestrial biosphere estimated from the Biome-BGC model (grey) and from atmospheric CO<sub>2</sub> measurements and modelling (green) [27].

# Observations clarify the carbon cycle of tropical regions: Amazonia as a net CO<sub>2</sub> source

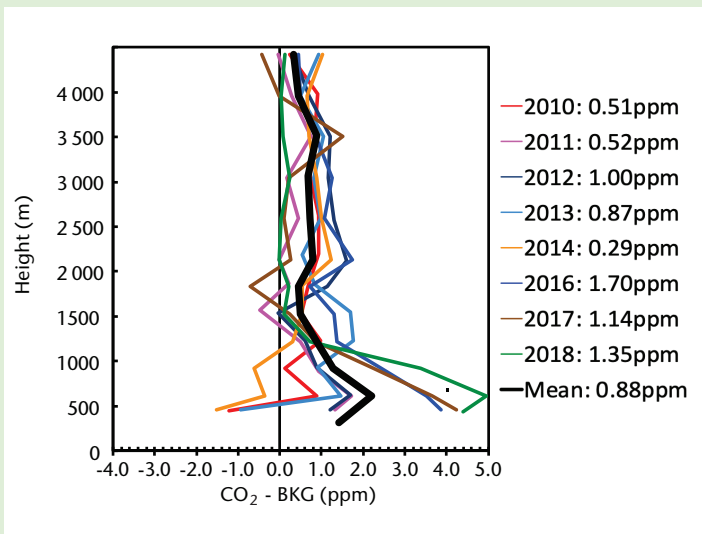


Figure 12. Annual mean vertical profiles at ALF aircraft measurement site in Brazil [28].

Tropical regions such as Amazonia play an important role in the global carbon balance. Amazonia hosts the Earth's largest tropical forest, but as with other tropical regions it has only a few of the in situ observations needed to determine the large-scale carbon fluxes. To improve estimates of Amazonia's contribution to the global carbon budget, an aircraft measurement programme was started in 2010 over four different sites in this region: Alta Floresta (ALF), Rio Branco (RBA), Santarém (SAN) and Tabatinga/Tefé (TAB/TEF). The vertical profiles extend from near the surface to approximately 4.5 km above sea level and the

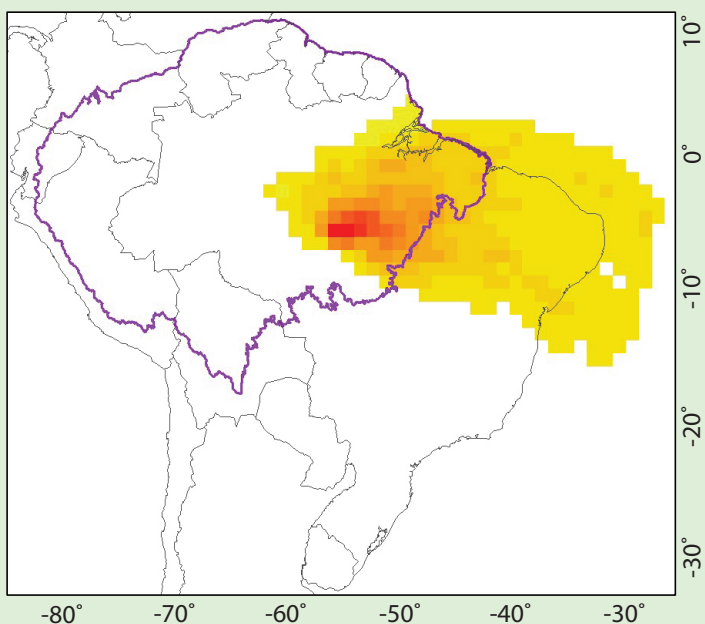


Figure 13. Footprint of the ALF aircraft measurement site (averaged area between 2010 and 2018).

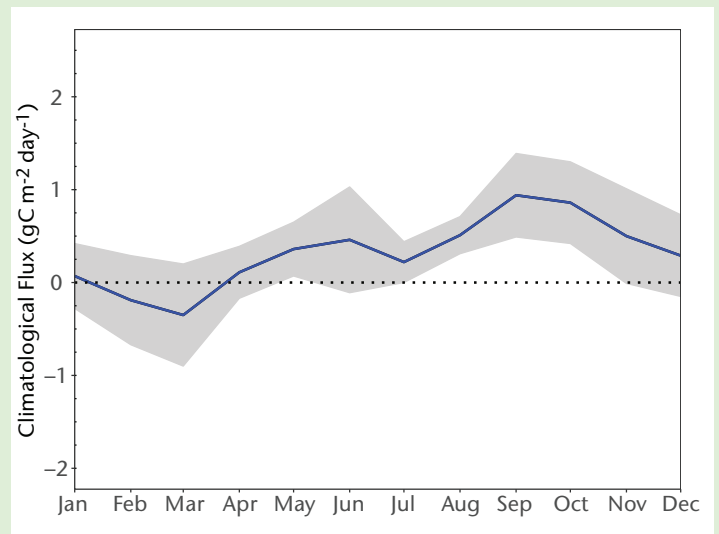


Figure 14. Average monthly means of ALF carbon fluxes during 2010–2018. The grey band denotes the standard deviation of the monthly means, and the solid line show 9-year mean climatological carbon flux at south-eastern Amazonia [28].

data gathered capture the surface flux balance from a large fraction of Amazonia (about 80% of South American Amazon). Overall, 600 CO<sub>2</sub> and CO aircraft vertical profiles have been collected between 2010 and 2018 [28].

Annual mean vertical profiles are shown in Figure 12. The south-east region, captured by the ALF site (8.80°S, 56.75°W; see Figure 13), has the largest CO<sub>2</sub> emissions to the atmosphere (Figure 14), followed by the north-east region. In contrast, the western sites' vertical gradients (not shown here) indicate near-neutral carbon balance or carbon sinks. The CO<sub>2</sub> gradients from the annual mean vertical profiles and the estimated carbon fluxes for these sites indicate that areas that are more affected by land-use and land-cover change show higher carbon emissions to the atmosphere. The regions in the eastern Amazon have very strong dry-season temperature increases, precipitation decreases and large historical deforestation during the last 40 years, while the western regions experience relatively low levels of human disturbance and dry-season climate trends.

in their abundances since 2019 and 1750. Data from mobile stations (blue triangles and orange diamonds in Figure 4), with the exception of data provided by NOAA sampling in the eastern Pacific, are not used for this global analysis.

The three GHGs, see the table, are closely linked to anthropogenic activities and interact strongly with the biosphere and the oceans. Predicting the evolution of the atmospheric content of GHGs requires a quantitative understanding of their many sources, sinks and chemical transformations in the atmosphere. Observations from GAW provide invaluable constraints on the budgets of these and other LLGHGs, and they are used to improve emission estimates and evaluate satellite retrievals of LLGHG column averages. The IG<sup>3</sup>IS provides further insights on the sources of GHGs at the national and subnational level.

The NOAA AGGI measures the increase in total radiative forcing due to all LLGHGs since 1990 [8]. The AGGI reached 1.47 in 2020, representing a 47% increase in total radiative forcing<sup>(4)</sup> from 1990 to 2020 and a 1.8% increase from 2019 to 2020 (Figure 3). The total radiative forcing by all LLGHGs in 2020 (3.18 W.m<sup>-2</sup>) corresponds to an equivalent CO<sub>2</sub> mole fraction of 504 ppm [8]. The relative contributions of other gases to the total radiative forcing since the pre-industrial era are presented in Figure 5.

## Carbon dioxide (CO<sub>2</sub>)

Carbon dioxide is the single most important anthropogenic GHG in the atmosphere, accounting for approximately 66%<sup>(4)</sup> of the radiative forcing by LLGHGs. It is responsible for about 82%<sup>(4)</sup> of the increase in radiative forcing over the past decade and also about 82% of the increase over the past five years. The pre-industrial level of 278 ppm represented a balance of fluxes among the atmosphere, the oceans and the land biosphere. The globally averaged CO<sub>2</sub> mole fraction in 2020 was 413.2 ± 0.2 ppm (Figure 6). The increase in annual means from 2019 to 2020 (2.5 ppm) was slightly lower than the increase from 2018 to 2019, but slightly higher than the average growth rate for the past decade (2.40 ppm yr<sup>-1</sup>), despite the approximately 5.6% drop in fossil fuel CO<sub>2</sub> emissions in 2020 due to restrictions related to the COVID-19 pandemic [13]. Note that the 2019 average global surface CO<sub>2</sub> reported in the sixteenth Greenhouse Gas Bulletin was adjusted from 410.5 ppm to 410.7 ppm due to the upgrade of all reported values to the new CO<sub>2</sub> X2019 calibration scale [12].

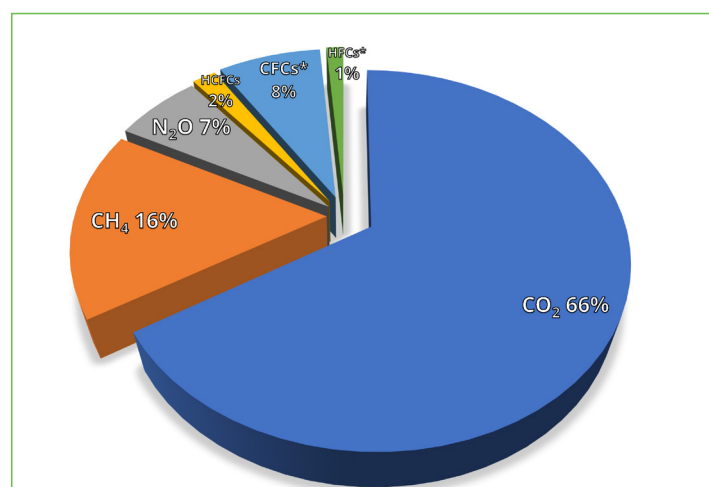


Figure 5. Contributions of the most important LLGHGs to the increase in global radiative forcing due to these gases from the pre-industrial era to 2020 [8].

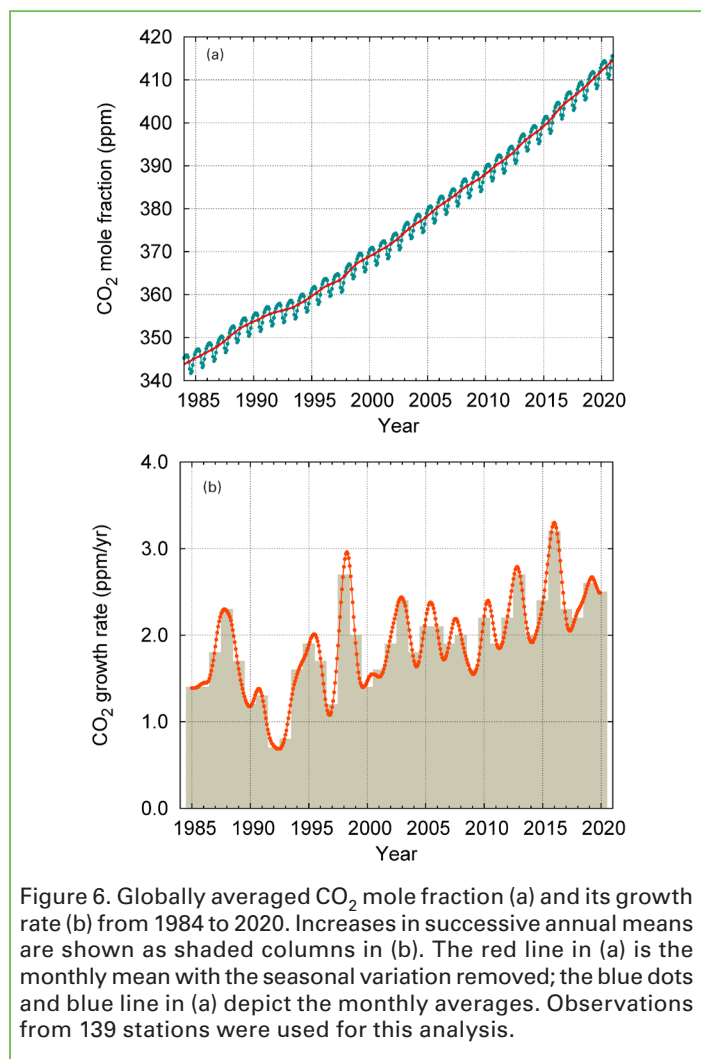


Figure 6. Globally averaged CO<sub>2</sub> mole fraction (a) and its growth rate (b) from 1984 to 2020. Increases in successive annual means are shown as shaded columns in (b). The red line in (a) is the monthly mean with the seasonal variation removed; the blue dots and blue line in (a) depict the monthly averages. Observations from 139 stations were used for this analysis.

In 2020, atmospheric CO<sub>2</sub> reached 149% of the pre-industrial level, primarily because of emissions from the combustion of fossil fuels and cement production. According to the International Energy Agency, fossil fuel CO<sub>2</sub> emissions reached 31.5 GtCO<sub>2</sub><sup>(5)</sup> in 2020, down from 33.4 GtCO<sub>2</sub> in 2019 [14]. According to the 2020 analysis of the Global Carbon Project, deforestation and other land-use change contributed 5.7 GtCO<sub>2</sub> yr<sup>-1</sup> (average for 2010–2019). Of the total emissions from human activities during the 2010–2019 period, about 46% accumulated in the atmosphere, 23% in the ocean and 31% on land, with the unattributed budget imbalance being 0.4% [15]. The portion of CO<sub>2</sub> emitted by fossil fuel combustion that remains in the atmosphere (airborne fraction) varies interannually due to the high natural variability of CO<sub>2</sub> sinks without a confirmed global trend (see also the cover story).

## Methane (CH<sub>4</sub>)

Methane accounts for about 16%<sup>(4)</sup> of the radiative forcing by LLGHGs. Approximately 40% of methane is emitted into the atmosphere by natural sources (for example, wetlands and termites), and about 60% comes from anthropogenic sources (for example, ruminants, rice agriculture, fossil fuel exploitation, landfills and biomass burning) [16]. Globally averaged CH<sub>4</sub> calculated from in situ observations reached a new high of 1889 ± 2 ppb in 2020, an increase of 11 ppb with respect to the previous year (Figure 7). This increase is higher than the increase of 8 ppb from 2018 to 2019 and higher than the average annual increase over the past decade. The mean annual increase of CH<sub>4</sub> decreased from approximately 12 ppb yr<sup>-1</sup> during the late 1980s to near zero during 1999–2006.

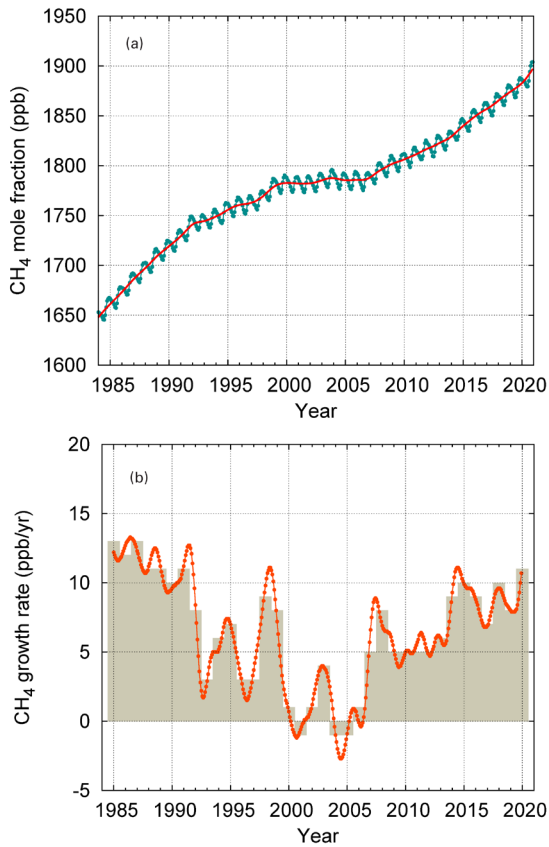


Figure 7. Globally averaged  $\text{CH}_4$  mole fraction (a) and its growth rate (b) from 1984 to 2020. Increases in successive annual means are shown as shaded columns in (b). The red line in (a) is the monthly mean with the seasonal variation removed; the blue dots and blue line in (a) depict the monthly averages. Observations from 138 stations were used for this analysis.

Since 2007, atmospheric  $\text{CH}_4$  has been increasing, and in 2020 it reached 262% of the pre-industrial level due to increased emissions from anthropogenic sources. Studies using GAW  $\text{CH}_4$  measurements indicate that increased  $\text{CH}_4$  emissions from wetlands in the tropics and from anthropogenic sources at the mid-latitudes of the northern hemisphere are the likely causes of this recent increase.

Recent studies have pointed to the short-term climate benefits and cost-effectiveness of mitigating  $\text{CH}_4$  emissions [17]. Some mitigation measures are presented in the United Nations Environment Programme (UNEP) methane assessment [18].

## Nitrous oxide ( $\text{N}_2\text{O}$ )

Nitrous oxide accounts for about 7%<sup>(4)</sup> of the radiative forcing by LLGHGs. It is the third most important individual contributor to the combined forcing. It is emitted into the atmosphere from both natural sources (approximately 60%) and anthropogenic sources (approximately 40%), including oceans, soils, biomass burning, fertilizer use and various industrial processes. The globally averaged  $\text{N}_2\text{O}$  mole fraction in 2020 reached  $333.2 \pm 0.1$  ppb, which is an increase of 1.2 ppb with respect to the previous year (Figure 8) and 123% of the pre-industrial level (270 ppb). The annual increase from 2019 to 2020 was higher than the increase from 2018 to 2019 and higher than the mean growth rate over the past 10 years ( $0.99 \text{ ppb yr}^{-1}$ ). Global human-induced  $\text{N}_2\text{O}$  emissions, which are dominated by nitrogen additions to croplands, increased by 30% over the past four decades to 7.3 (range: 4.2–11.4) teragrams of nitrogen per year. Agriculture,

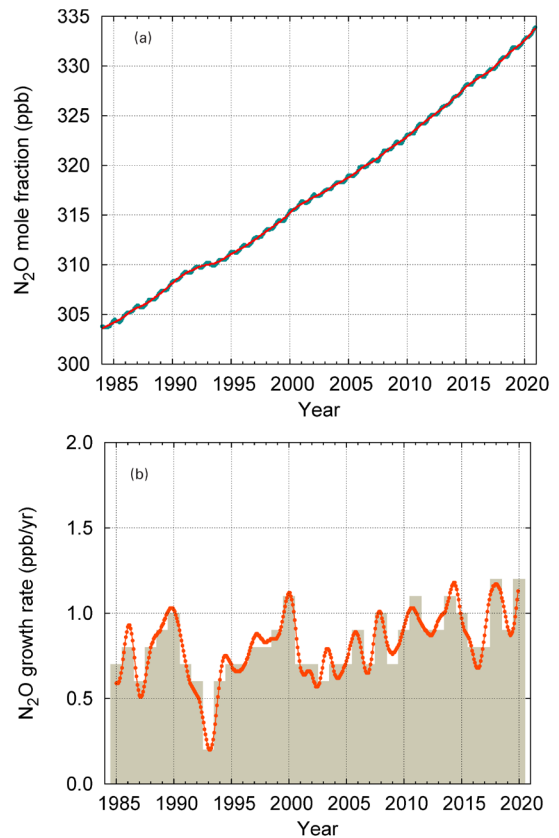


Figure 8. Globally averaged  $\text{N}_2\text{O}$  mole fraction (a) and its growth rate (b) from 1984 to 2020. Increases in successive annual means are shown as shaded columns in (b). The red line in (a) is the monthly mean with the seasonal variation removed; in this plot, the red line overlaps the blue dots and blue line that depict the monthly averages. Observations from 105 stations were used for this analysis.

owing to the use of nitrogen fertilizers and manure, contributes 70% of all anthropogenic  $\text{N}_2\text{O}$  emissions. This increase was mainly responsible for the growth in the atmospheric burden of  $\text{N}_2\text{O}$  [19].

## Other greenhouse gases

The stratospheric ozone-depleting CFCs, which are regulated by the Montreal Protocol on Substances that Deplete the Ozone Layer, together with minor halogenated gases, account for approximately 11%<sup>(4)</sup> of the radiative forcing by LLGHGs. While CFCs and most halons are decreasing, some HCFCs and HFCs, which are also potent GHGs, are increasing at relatively rapid rates, although they are still low in abundance (at ppt<sup>(6)</sup> levels). The current observational network for CFCs is insufficient to determine important emission sources in a timely manner [20]. Although at a similarly low abundance,  $\text{SF}_6$  is an extremely potent LLGHG. It is produced by the chemical industry, mainly as an electrical insulator in power distribution equipment. Its current mole fraction is more than twice the level observed in the mid-1990s (Figure 9(a)).

This Bulletin primarily addresses LLGHGs. Relatively short-lived tropospheric ozone has a radiative forcing comparable to that of the halocarbons [21]. Many other pollutants, such as carbon monoxide (CO), nitrogen oxides and volatile organic compounds, although not referred to as GHGs, have small direct or indirect effects on radiative forcing [9]. Aerosols (suspended particulate matter) are short-lived substances that alter the radiation budget. All the gases mentioned in this Bulletin, as well as aerosols, are included in the observational

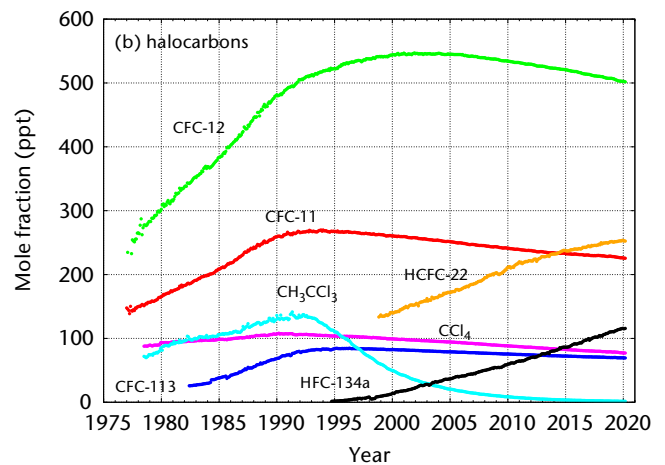
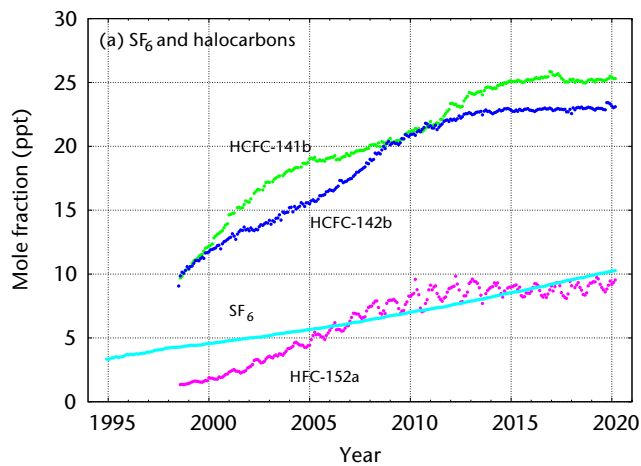


Figure 9. Monthly mean mole fractions of SF<sub>6</sub> and the most important halocarbons: (a) SF<sub>6</sub> and lower mole fractions of halocarbons and (b) higher halocarbon mole fractions. For each gas, the number of stations used for the analysis was as follows: SF<sub>6</sub> (88), CFC-11 (23), CFC-12 (25), CFC-113 (22), CCl<sub>4</sub> (22), CH<sub>2</sub>Cl<sub>2</sub> (25), HCFC-141b (10), HCFC-142b (15), HCFC-22 (14), HFC-134a (11) and HFC-152a (10).

programme of GAW, with support from WMO Members and contributing networks [22].

## Acknowledgements and links

Fifty-five WMO Members contributed CO<sub>2</sub> and other GHG data to the GAW WDCGG. Approximately 40% of the measurement records submitted to WDCGG were obtained at sites of the NOAA Global Monitoring Laboratory cooperative air-sampling network. For other networks and stations, see GAW Report No. 255 [23]. The Advanced Global Atmospheric Gases Experiment also contributed observations to this Bulletin. The GAW observational stations that contributed data to this Bulletin (see Figure 4) are included in the list of contributors on the WDCGG web page (<https://gaw.kishou.go.jp>). They are also described in the GAW Station Information System, GAW SIS (<http://gawsis.meteoswiss.ch>), supported by MeteoSwiss, Switzerland. The Bulletin is prepared under the oversight of the GAW Scientific Advisory Group on Greenhouse Gases.

## Editorial board

Alex Vermeulen (Integrated Carbon Observation System - European Research Infrastructure Consortium (ICOS ERIC)/Lund University, Sweden), Yousuke Sawa (Japan Meteorological Agency, WDCGG, Japan), Oksana Tarasova (WMO)

## Authors (in alphabetical order)

Luana Basso (National Institute for Space Research, Brazil), Andy Crotwell (NOAA Global Monitoring Laboratory and Cooperative Institute for Research in Environmental Sciences, University of Colorado Boulder, United States of America), Han Dolman (Vrije Universiteit Amsterdam, Netherlands), Luciana Gatti (National Institute for Space Research, Brazil), Christoph Gerbig (Max Planck Institute for Biogeochemistry, Germany), David Griffith (University of Wollongong, Australia), Bradley Hall (NOAA Global Monitoring Laboratory, United States of America), Armin Jordan (Max Planck Institute for Biogeochemistry, Germany), Paul Krummel (Commonwealth Scientific and Industrial Research Organisation, Australia), Markus Leuenberger (University of Bern, Switzerland), Zoë Loh (Commonwealth Scientific and Industrial Research Organisation, Australia), Sara Mikaloff-Fletcher (GNS Science, Manaaki Whenua – Landcare Research, and University of Waikato, New Zealand), Yousuke Sawa (Japan Meteorological Agency, WDCGG, Japan), Michael Schibig (University of Bern,

Switzerland), Oksana Tarasova (WMO), Jocelyn Turnbull (GNS Science, New Zealand/Cooperative Institute for Research in Environmental Sciences, University of Colorado Boulder, United States of America), Alex Vermeulen (ICOS ERIC/Lund University, Sweden).

## References

- [1] Bennedsen, M., E. Hillebrand and S.J. Koopman, 2019: Trend analysis of the airborne fraction and sink rate of anthropogenically released CO<sub>2</sub>. *Biogeosciences*, 16: 3651–3663, <https://doi.org/10.5194/bg-16-3651-2019>.
- [2] Ciavarella, A. et al., 2021: Prolonged Siberian heat of 2020 almost impossible without human influence. *Climatic Change*, 166: 9, <https://doi.org/10.1007/s10584-021-03052-w>.
- [3] Jiang, L.Q., et al., 2019. Surface ocean pH and buffer capacity: past, present and future. *Scientific Reports*, 9: 18624, <https://doi.org/10.1038/s41598-019-55039-4>.
- [4] Caesar, L. et al., 2021: Current Atlantic Meridional Overturning Circulation weakest in last millennium. *Nature Geoscience*, 14: 118–120, <https://doi.org/10.1038/s41561-021-00699-z>.
- [5] Manning, A. and R.F. Keeling, 2006: Global oceanic and land biotic carbon sinks from the Scripps atmospheric oxygen flask sampling network. *Tellus B: Chemical and Physical Meteorology*, 58(2): 95–116, <https://doi.org/10.1111/j.1600-0889.2006.00175.x>.
- [6] GCOS, 2021: The Status of the Global Climate Observing System 2021: *The GCOS Status Report*, (GCOS-240), WMO, Geneva.
- [7] Schibig, M.F., 2015: Carbon and oxygen cycle related atmospheric measurements at the terrestrial background station Jungfraujoch. PhD thesis, University of Bern.
- [8] Butler, J.H. and S.A. Montzka, 2020: The NOAA Annual Greenhouse Gas Index (AGGI). NOAA, Earth System Research Laboratories, Global Monitoring Laboratory, <http://www.esrl.noaa.gov/gmd/aggi/aggi.html>.
- [9] IPCC, 2021: *Climate Change 2021: The Physical Science Basis. Contribution of Working Group I to the Sixth Assessment Report of the Intergovernmental Panel on Climate Change* (V. Masson-Delmotte et al., eds.). Cambridge University Press, <https://www.ipcc.ch/report/sixth-assessment-report-working-group-i/>.
- [10] NOAA, Earth System Research Laboratories, Global Monitoring Laboratory, 2020: Trends in atmospheric carbon dioxide, <http://www.esrl.noaa.gov/gmd/ccgg/trends/>.
- [11] Tsutsumi, Y. et al., 2009: *Technical Report of Global Analysis Method for Major Greenhouse Gases by the World Data Center for Greenhouse Gases* (WMO/TD-No. 1473). GAW Report No. 184. Geneva, WMO, [https://library.wmo.int/index.php?lvl=notice\\_display&id=12631](https://library.wmo.int/index.php?lvl=notice_display&id=12631).

- [12] Hall, B.D. et al., 2021: Revision of the World Meteorological Organization Global Atmosphere Watch (WMO/GAW) CO<sub>2</sub> calibration scale. *Atmospheric Measurement Techniques*, 14: 3015–3032, <https://doi.org/10.5194/amt-14-3015-2021>.
- [13] Le Quéré, C. et al., 2020: Temporary reduction in daily global CO<sub>2</sub> emissions during the COVID-19 forced confinement. *Nature Climate Change*, 10: 647–653, <https://doi.org/10.1038/s41558-020-0797-x>.
- [14] International Energy Agency, 2021: Global energy review: CO<sub>2</sub> emissions in 2020, <https://www.iea.org/articles/global-energy-review-co2-emissions-in-2020>.
- [15] Friedlingstein, P. et al., 2020: Global Carbon Budget 2020. *Earth System Science Data*, 12(4): 3269–3340, <https://doi.org/10.5194/essd-12-3269-2020>.
- [16] Saunio, M. et al., 2020: The Global Methane Budget 2000–2017. *Earth System Science Data*, 12(3): 1561–1623, <https://doi.org/10.5194/essd-12-1561-2020>.
- [17] Nisbet, E.G. et al., 2020: Methane mitigation: methods to reduce emissions, on the path to the Paris Agreement. *Reviews of Geophysics*, 58(1): e2019RG000675, <https://doi.org/10.1029/2019RG000675>.
- [18] UNEP and Climate and Clean Air Coalition, 2021: *Global Methane Assessment: Benefits and Costs of Mitigating Methane Emissions*. Nairobi, UNEP, <https://www.unep.org/resources/report/global-methane-assessment-benefits-and-costs-mitigating-methane-emissions>.
- [19] Tian, H. et al., 2020: A comprehensive quantification of global nitrous oxide sources and sinks. *Nature*, 586: 248–256, <https://doi.org/10.1038/s41586-020-2780-0>.
- [20] Weiss, R.F., A.R. Ravishankara and P.A. Newman, 2021: Huge gaps in detection networks plague emissions monitoring. *Nature*, 595: 491–493, <https://doi.org/10.1038/d41586-021-01967-z>.
- [21] WMO, 2018: *WMO Reactive Gases Bulletin: Highlights from the Global Atmosphere Watch Programme*, No. 2, [https://library.wmo.int/index.php?lvl=notice\\_display&id=20667#YWcnpbj0njZ](https://library.wmo.int/index.php?lvl=notice_display&id=20667#YWcnpbj0njZ).
- [22] WMO, 2021: *WMO Air Quality and Climate Bulletin*, No. 1, [https://library.wmo.int/index.php?lvl=notice\\_display&id=21942](https://library.wmo.int/index.php?lvl=notice_display&id=21942).
- [23] WMO, 2020: *20th WMO/IAEA Meeting on Carbon Dioxide, Other Greenhouse Gases and Related Measurement Techniques* (GGMT-2019). GAW Report No. 255. Geneva, [https://library.wmo.int/doc\\_num.php?explnum\\_id=10353](https://library.wmo.int/doc_num.php?explnum_id=10353).
- [24] Henne, S. et al., 2008: Mount Kenya Global Atmosphere Watch station (MKN): installation and meteorological characterization. *Journal of Applied Meteorology and Climatology*, 47(11): 2946–2962, <https://doi.org/10.1175/2008jamc1834.1>.
- [25] New Zealand Ministry for the Environment, 2021: *New Zealand's Greenhouse Gas Inventory 1990-2019* Wellington, <https://environment.govt.nz/publications/new-zealands-greenhouse-gas-inventory-1990-2019/>.
- [26] IPCC, 2019: 2019 *Refinement to the 2006 IPCC Guidelines for National Greenhouse Gas Inventories*, <https://www.ipcc.ch/report/2019-refinement-to-the-2006-ipcc-guidelines-for-national-greenhouse-gas-inventories/>.
- [27] Steinkamp, K. et al., 2017: Atmospheric CO<sub>2</sub> observations and models suggest strong carbon uptake by forests in New Zealand. *Atmospheric Chemistry and Physics*, 17(1): 47–76, <https://acp.copernicus.org/articles/17/47/2017/>.
- [28] Gatti, L.V. et al., 2021: Amazonia as a carbon source linked to deforestation and climate change. *Nature*, 595: 388–393, <https://doi.org/10.1038/s41586-021-03629-6>.

## Contacts

World Meteorological Organization  
 Atmospheric Environment Research Division  
 Science and Innovation Department  
 Geneva, Switzerland  
 Email: [gaw@wmo.int](mailto:gaw@wmo.int)  
 Website: <https://community.wmo.int/activity-areas/gaw>

World Data Centre for Greenhouse Gases  
 Japan Meteorological Agency  
 Tokyo, Japan  
 Email: [wdcgg@met.kishou.go.jp](mailto:wdcgg@met.kishou.go.jp)  
 Website: <https://gaw.kishou.go.jp>

### Notes:

- (1) Mole fraction = the preferred expression for the abundance (concentration) of a mixture of gases or fluids. In atmospheric chemistry, the mole fraction is used to express the concentration as the number of moles of a compound per mole of dry air.
- (2) ppm = the number of molecules of the gas per million (10<sup>6</sup>) molecules of dry air
- (3) ppb = the number of molecules of the gas per billion (10<sup>9</sup>) molecules of dry air
- (4) This percentage is calculated as the relative contribution of the mentioned gas(es) to the increase in global radiative forcing caused by all LLGHGs since 1750.
- (5) 1 GtCO<sub>2</sub> = 1 billion (10<sup>9</sup>) metric tons of carbon dioxide
- (6) ppt = the number of molecules of the gas per trillion (10<sup>12</sup>) molecules of dry air

# Selected greenhouse gas observatories

## Mount Kenya (MKN)



Photo: WMO

The Mount Kenya GAW site (station identifier MKN) is located on the north-western slope of Mount Kenya close to the Sirimon route and about 5 km south-west and 200 m below Timau Hill [24]. It is operated by the Kenya Meteorological Department, Nairobi. The mission of the station is to perform long-term measurements of GHGs and aerosols in equatorial Africa and to assess the contribution of agricultural burning and forest-clearing activities to the build-up of regional ozone. Mount Kenya is an isolated, almost conical mountain of volcanic origin, which rises moderately from the surrounding foreland (1 800–2 000 metres above sea level (m a.s.l)) to about 4 300 m a.s.l. The area has been protected since 1949 as part of Mount Kenya National Park and was designated a World Heritage Site in 1997.

The station was designed as a mobile two-container building that was completely equipped and taken into operation in Germany by the Forschungszentrum Karlsruhe (FZK) Institute for Meteorology and Climate Research–Atmospheric Environmental Research. It was shipped as a whole unit to Kenya. The station was officially inaugurated in October 1999. Cooperative flask sampling started with the NOAA Global Monitoring Laboratory for the analysis of CO, CO<sub>2</sub>, N<sub>2</sub>O, CH<sub>4</sub>, H<sub>2</sub>, SF<sub>6</sub> and the isotopes of hydrogen and oxygen. Instrument calibration is done biennially by the Swiss Federal Laboratories for Materials Testing and Research (EMPA). Power to the station is provided by a 26-km overland power line passing through the tropical forest.

### Location

Country: Kenya  
 Latitude: 0.0622° South  
 Longitude: 37.2922° East  
 Elevation: 3 644 m asl  
 Time zone: Local time = UTC +3



## Barrow (BRW)



Photo: NOAA

Officially established in 1973, the Barrow Atmospheric Baseline Observatory (BRW) is NOAA's northernmost station and the longest continuously operating atmospheric climate observatory in the Arctic. Located 8 km north-east of the city of Utqiagvik (formerly Barrow), Alaska, BRW is purposely situated upwind of human habitation, in an isolated area which allows for the monitoring of air that has not been affected by regional air pollution sources.

The original 74 m<sup>2</sup> observatory building was built in 1973 and has hosted numerous long-term climate-related measurements and campaign-style experiments during its tenure. After 47 years, the structure no longer met the needs of researchers and was replaced in 2020 with a new 273 m<sup>2</sup> main building and support structures. The new facility includes a roof deck, a 30-m instrument tower, a campaign science platform that can hold two 6-m metal shipping containers and a high-speed fibre connection to the contiguous United States equipment that was transitioned to the new building in late 2020. Today, BRW supports more than 200 measurements enabling research on atmospheric composition, climate, solar radiation, aerosols and stratospheric ozone.



### Location

Country: USA  
 Latitude: 71.323° North  
 Longitude: 156.611° West  
 Elevation: 11 m asl  
 Time zone: Local time = UTC – 9

